Morphology of Solution-grown Crystals and Crystalline Thin Films of Poly (p-phenylene sulfide)

AUTHOR(S):

Uemura, Akio; Isoda, Seiji; Tsuji, Masaki; Ohara, Masayoshi; Kawaguchi, Akiyoshi; Katayama, Ken-ichi

Bull. Inst. Chem. Res., Kyoto Univ., Vol. 64, No. 2, 1986

Morphology of Solution-grown Crystals and Crystalline Thin Films of Poly (*p*-phenylene sulfide)

Akio UEMURA, Seiji ISODA, Masaki TSUJI, Masayoshi OHARA, Akiyoshi KAWAGUCHI, and Ken-ichi KATAYAMA

Received May 12, 1986

Poly(*p*-phenylene sulfide) (PPS) was dissolved in α-chloronaphthalene in a concentration of 0.1 wt%, and crystallized isothermally at 167°C. The fibrillar morphology of PPS solution-grown crystal was observed under an electron microscope. The electron diffraction from the specimen revealed that the growing direction of these fibrillar crystals is parallel to the **b**-axis. It was also found that the fibrillar crystals grow changing their orientation around the **b**-axis. With an electron microscope operated at the accelerating voltage of 200 kV, the high resolution image of this crystal was obtained. This image consists of the lattice fringes corresponding to three lattice planes; (200), (110), and (110). The micrograph (original negative) was image-processed with the optical filtering method to improve signal-to-noise ratio, and was compared with the image simulated by a computer.

A crystalline thin film of PPS with the spherulitic structure was obtained by casting 1 wt% solution. The spherulite in this film is optically negative. At the center and its neighbourhood of a spherulite the molecular axis (**c**-axis) is normal to the surface of the film. At other places of the spherulite, the **b**-axis and the **c**-axis are basically parallel to the radial and the tangential directions, respectively.

KEY WORDS: Poly(*p*-phenylene sulfide)/ High resolution electron microscopy/ Spherulite/ Solution-grown crystal/

INTRODUCTION

Poly(*p*-phenylene sulfide) (PPS) has rather high thermostability and small molding contraction. Owing to these characteristics, PPS is used in the electric and electronic field, machinery field and so on.[1] PPS has a glass transition point of about 90°C and a melting point of about 280°C. The crystal structure of PPS has already been analyzed and the unit cell is orthorhombic with the cell dimensions: **a**= 0.867 nm, **b**=0.561 nm, and **c**=1.026 nm (**c**-axis is the chain axis).[2] The electroconducting mechanism of doped PPS has been discussed by many workers, but the morphology of PPS itself and doped PPS has not been studied very well.

We have studied the morphologies of fibers or fibrils of polyethylene, poly(*p*-phenylene terephthalamide), (SN)x, isotactic polystyrene, poly(*p*-xylylene), poly(*p*-phenylene) and so on by electron microscopy.[3,4,5,6] The structure analysis of poly(*p*-xylylene) β-form crystal was finally achieved being based on the molecular image by high resolution electron microscopy.[5] It was also found by high resolution electron microscopy that (SN)x microfibril has 'skin-core' structure, and that when (SN)x was doped with iodine, iodine atoms invade and are structurized preferentially in its 'skin'

植村明夫, 磯田正二, 辻　正樹, 小原正義, 河口昭義, 片山健一 : Laboratory of Polymer Crystals, Institute for Chemical Research, Kyoto University, Uji, Kyoto-fu, 611.

region which is disordered in the pristine state.[7,8] Thus high resolution electron microscopy has become one of powerful techniques to investigate the very fine structure even in the field of polymer science.

We have obtained solution-grown crystals and crystalline thin films with the spherulitic structure of PPS. In this paper, the morphologies of these specimens studied by polarizing light microscopy and electron microscopy, especially by high resolution electron microscopy are presented.

EXPERIMENTAL

1. Sample preparation

As a sample of PPS, Ryton, manufactured by Phillips Petroleum Company, was used.

a) *Solution-grown crystals*

Ryton V-1 was dissolved in α-chloronaphthalene in a concentration of 0.1 wt%, and allowed to stand for a few days at 167°C. Then the crystals were precipitated.

b) *Crystalline thin films with spherulitic structure*

Ryton V-1 was dissolved in α-chloronaphthalene in a concentration of 1 wt%. This solution was dropped on the surface of a slide glass set on a hot-plate whose temperature was regulated about 300°C. A drop of the solution was spread on the slide glass. After evaporation of the solvent or in the state that the solvent is slightly contained, the melt was elongated into a thin film by sliding another slide glass. After complete evaporation of the solvent, temperature was lowered. A crystalline thin film with the spherulitic structure was thus obtained on the slide glass.

2. Optical microscopy

The crystalline thin films with spherulitic structure were observed, in advance of electron microscopy, under an optical microscope between crossed polars with or without a sensitive colour plate.

3. Electron microscopy

Solution-grown crystals were deposited on a carbon-coated Cu-grid for electron microscopy. Crystalline thin films adhered tightly to a slide glass was immersed into the diluted HF aqueous solution and floated off from the slide glass on the water surface. The thin film was directly picked up on a Cu-grid.

Morphological observation and electron diffraction experiments of these PPS samples were carried out using JEOL JEM-200CS (200 kV) and JEM-7A (80 kV) electron microscopes. High resolution images of the solution-grown crystal were obtained using JEM-200CS (200 kV) equipped with a minimum dose system (MDS).[9]

4. Small angle X-ray scattering

The thickness of the solution-grown crystal was evaluated by small angle X-ray scattering of a sedimented mat of the crystal. Rigaku RU-3H was used as an X-ray source.

RESULTS AND DISCUSSION

1) *Solution-grown crystals*

Figures 1 and 2 show an electron micrograph and a corresponding electron

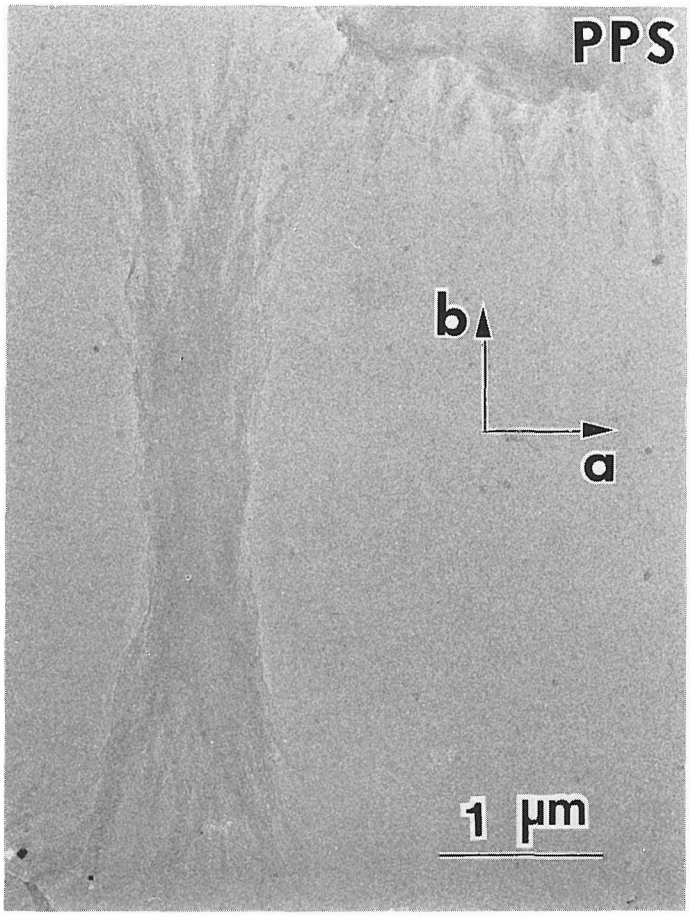

Fig. 1. Solution-grown crystal of PPS (without shadowing).

diffraction pattern of the solution-grown crystal, respectively. Fibrillar crystals with the width of 30–40 nm grow along the **b**-axis. The thickness of this crystal was measured to be 11.5 nm from the small angle X-ray scattering of a sedimented mat of the crystal. In the electron micrograph of the crystal shadowed with Pt-Pd, several 'microfibrillar' crystals seem to exist in a fibrillar crystal. At present, however, detailed morphology of individual 'microfibrillar' crystals is obscure and further study must be waited for.

The electron diffraction pattern (Fig. 2) of the fibrillar crystal shows *hk*0 reflections such as 200, 110 and 020. These reflections arced but are located to be put on the *hk*0 reciprocal lattice net. From this, it is found that the molecular axis (**c**-axis) is fundamentally normal to the basal plane of the solution-grown crystal (the incident electron beam is parallel to the **c**-axis). However, the *hkℓ* reflections with $\ell \neq 0$ such as 111 and 211 reflections are also observed in the diffraction pattern of Fig. 2 (see the reflections arrowed in the figure 2). The structure in which the molecular axis is normal to the basal plane of the crystal does not give the reflections such as 111, when

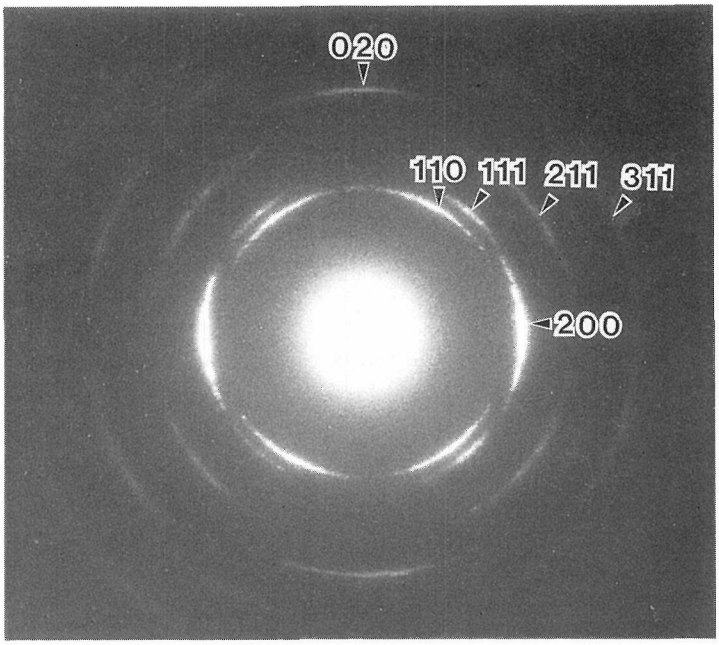

Fig. 2. Electron diffraction pattern of a PPS solution-grown crystal corresponding to Fig. 1.

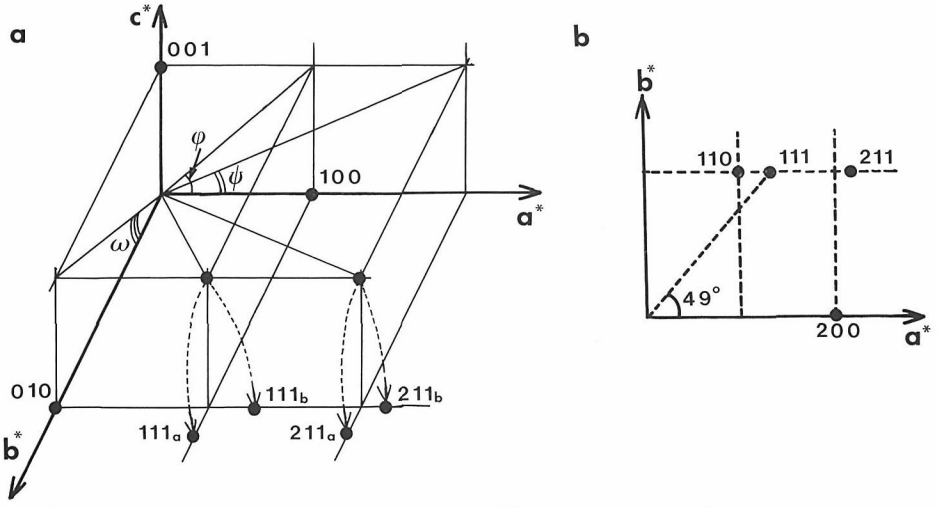

Fig. 3. Ewald construction of reflection. (a) When the crystal is tilted at the angle of 40.2° (φ) around the **b**-axis, the 111 reflection appears at the position indicated with 111_b, and when tilted at the angle of 22.9° (ψ) around the **b**-axis, the 211 reflection appears at 211_b. When the crystal is tilted at the angle of 28.7° (ω) around the **a**-axis, 111_a and 211_a appear. (b) Only **a***-**b*** plane is illustrated.

the incident electron beam is parallel to the **c**-axis. It is considered that both the portion of crystal giving *hk*0 reflections and the portion which produces the reflections of 111, 211 and so on coexist in the small area selected by an aperture (its diameter

corresponds to 500 nm on the specimen) of an electron microscope. The complicated diffraction pattern can be interpreted with the help of the Ewald construction of reflection as follows.

Figure 3(a) shows schematically the Ewald construction of reflection. When the incidence of electron beam is parallel to the **c**-axis, only the *hk*0 reciprocal points are put on the reflection sphere of Ewald (the plane normal to the direction of electron beam) and then these reflections can be observed. Since the 111 and 211 reciprocal points are far off from the sphere of reflection in the condition, however, these reflections do not appear. When the crystal is tilted at an angle of 40.2° around the **b**-axis, the 111 reflection is able to be observed, that is, the 111 reciprocal point is put on the sphere by the rotation of the reciprocal lattice around the **b***-axis by this angle.

Figure 3(b) shows the geometrical relation of the 111 reflection to *hk*0 reflections. It is quite similar to the real electron diffraction pattern. The 211 reflection appears when the crystal is tilted at an angle of 22.9°. Thus, the electron diffraction pattern

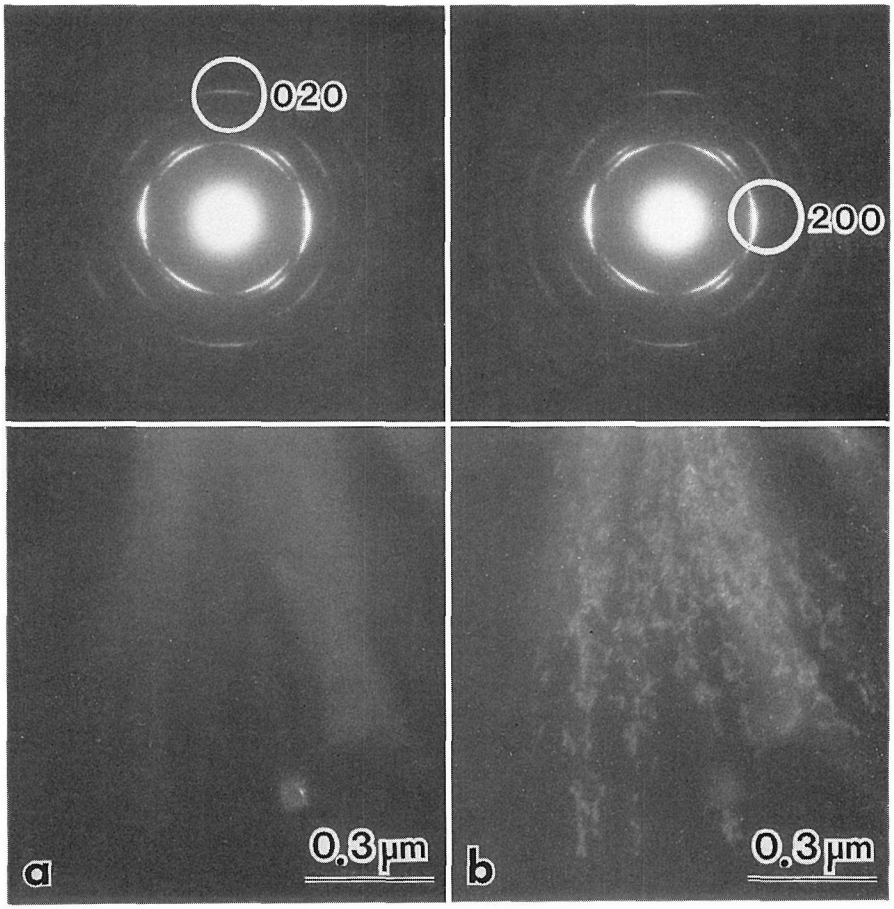

Fig. 4. (a) Dark-field image taken with the 020 reflection. (b) the 200 dark-field image of the same specimen-portion that was used for (a). As the 020 reflection is weak, (a) was taken in advance of (b).

of Fig. 2 including extra-reflections such as 111, 211, etc. is able to be explained by some distribution of fibrillar PPS crystals and/or the portions of them around the **b**-axis, with their **c**-axis within an angle of 40.2° from the normal. As a matter of fact, in the observation under an electron microscope neither 200 nor 111 reflection disappeared even by tilting the specimen up to about 30° around the **b**-axis. The dark field images with 020 and 200 reflections are shown in Fig. 4(a) and (b), respectively. The bright dots are studded in the dark field image of 200 reflection. The (200) plane is not always parallel to the incident electron beam. To the contrary, the image of 020 reflection has uniform brightness over the whole area of the crystal. From these results, it is considered that crystals may consist of many fibrillar crystals which keep their **b**-axis perpendicular to the direction of incident electron beam, though changing their orientation around the **b**-axis.

Total end point dose (TEPD, the electron irradiation dose which is needed for crystals to lose the crystalline reflections in the diffraction pattern) of PPS crystal was measured as about 0.2 C/cm^2 at an accelerating voltage of 200 kV. Generally, polymers are weak to the electron bombardment, but PPS is rather strong against electron radiation. Hence the high resolution electron microscopic image of this crystal was expected and really we succeeded in obtaining it. Figure 5 shows the high resolution image of PPS with 200 (0.43 nm in spacing), 110 (0.47 nm) and $\bar{1}10$ (0.47 nm) lattice fringes. The optical diffraction obtained by optical-transformation of the original negative is inset in Fig. 6. From this optical diffraction, it is confirmed that the fringes recorded onto the negative were 200, 110 and $\bar{1}10$ lattice fringes. As seen in Fig. 5, the image is blurred due to the low signal-to-noise ratio which results mainly from the granularity of recording film. The clear spots of the optical diffractogram of Fig. 6 shows surely, however, that the lattice images are recorded on the original negative. In order to enhance the periodic structure in the images, the image-processing was performed using the optical filtering method (Fig. 6).[10] Now as the molecular chain is normal to the crystal surface, each ellipse of the processed image corresponds to a molecular chain projected on the **a**–**b** plane along the chain direction. Taking account of the parameters of the crystal structure[2] and the characteristics of the electron microscope (JEM-200CS), the molecular image projected along the chain axis was simulated by a computer on the assumption of kinematical diffraction.[11] It is shown at the upper left-hand corner of the Fig. 6. This simulated image is well coincident with the electron microscopic image.

Sometimes the diffraction pattern shown in Fig. 7 is observed. The *h*11 and *h*00 reflections are seen in Fig. 7, but 110 and 020 reflections are not. Figure 8 shows the geometrical relationship between these reflections and *hk*0 ones on the **a***–**b*** plane. It is impossible that all these reflections appear at the same time, when crystallites have the same orientation. As discussed in the case of Fig. 3, the distribution of the orientation of crystallites must be taken into account. On the basis of Ewald construction of reflection in Fig. 3 (a), the diffraction pattern can be interpreted as follows. When the crystals are tilted at the angle of 28.7° around the **a**-axis, the 111 reciprocal point is put on the reflection sphere and then the 020 and 110 reflections are off from it. Thus, the 111 reflection appears and the 020 and 110 reflections can

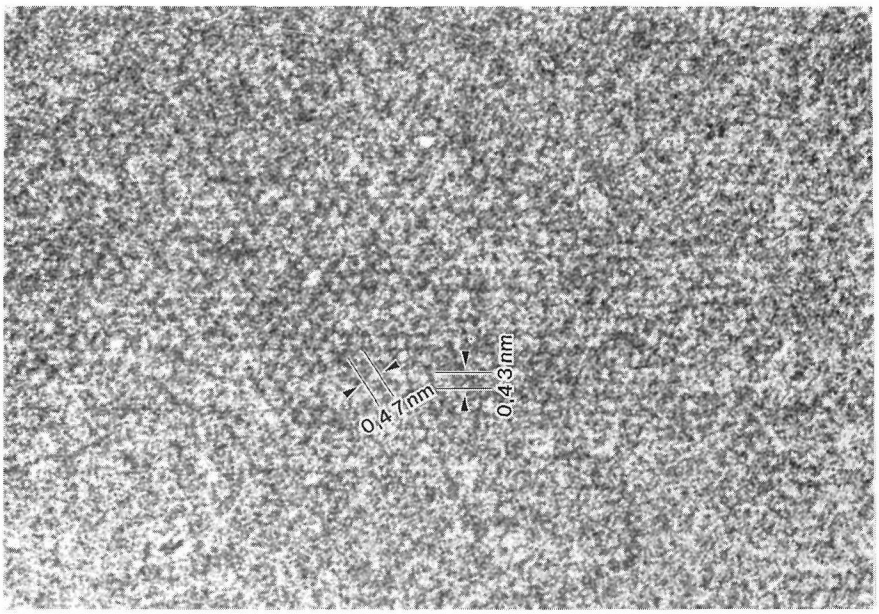

Fig. 5. High resolution image of a PPS solution-grown crystal. Fringes of 0.47 nm and 0.43 nm are observed and these correspond to (200) and (110) spacings.

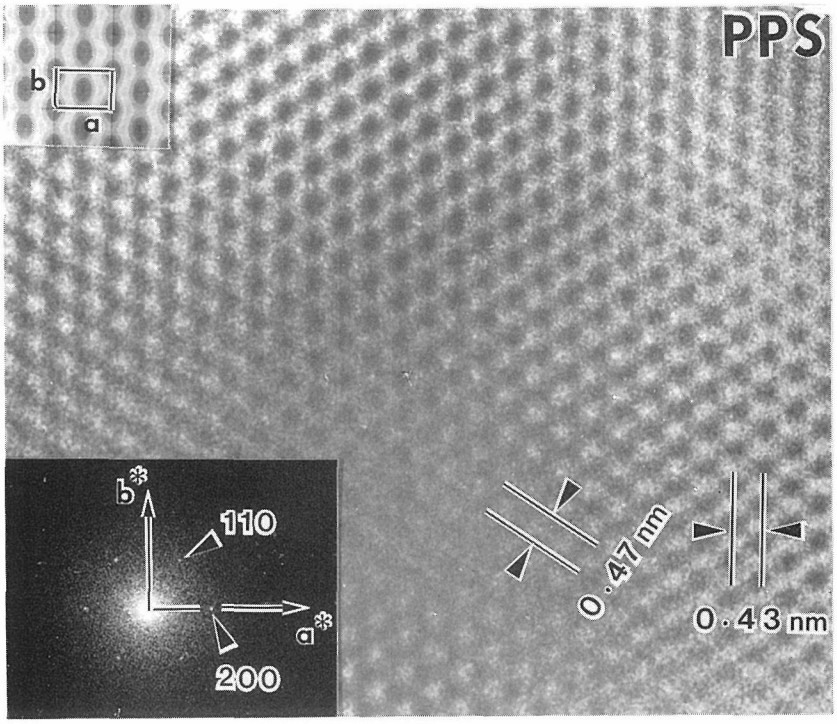

Fig. 6. Optically filtered high resolution image of a PPS solution-grown crystal. Inset is the optical diffractogram of the respective image. The molecular image simulated by a computer is also shown at the upper left-hand corner. Simulation conditions are as follows: spherical aberration coefficient 2.8 mm, amount of defocus 90 nm (under focus).

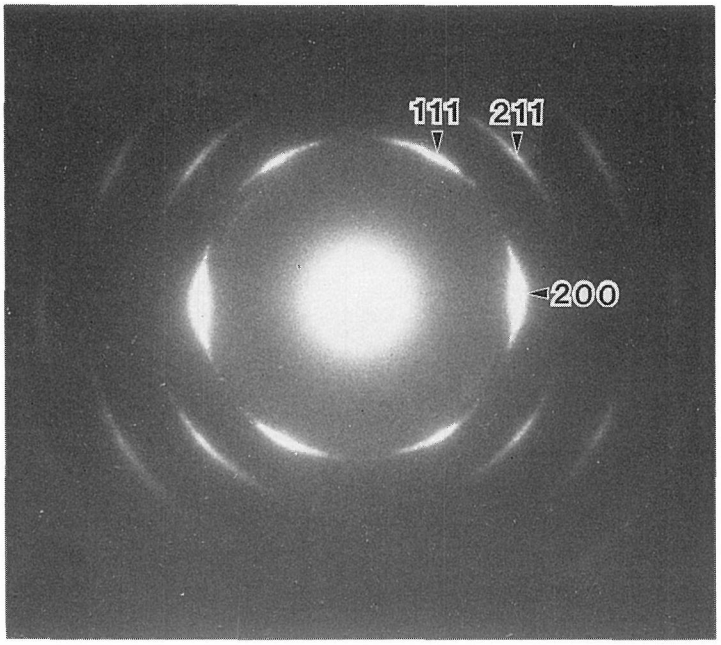

Fig. 7. Electron diffraction pattern of a PPS solution-grown crystal. The 110 and 020 reflections are off from it, and the 111 reflection appears at the different position from that of Fig. 2.

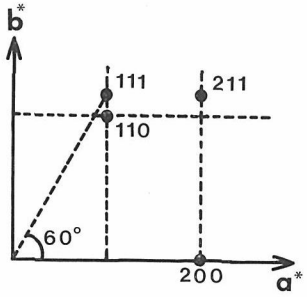

Fig. 8. Ewald construction of reflection.

not be observed. The positional relationship of the 111 reflection produced by this way to the original 110 reflection was schematically indicated in Fig. 8. The position of 111 reflection in the present diffraction pattern is different from that of 111 reflection in the case of tilting around **b***-axis (compare Fig. 7 with Fig. 2, or Fig. 8 with Fig. 3(b)). It was practically observed under the electron microscope that 110 and 020 reflections disappeared and the intensity of 111 reflection increased by tilting the specimen at the angle of about 30° around the **a**-axis. The observation proves the above consideration. So the fibrillar crystals occasionally tilt around the **a**-axis by undifined reasons.

High resolution electron micrographs were obtained from a specimen with the above orientation of chains. Figure 9 shows the optical diffraction pattern of the micrograph, and 200, 111 and 211 reflections are seen. Since this optical diffraction

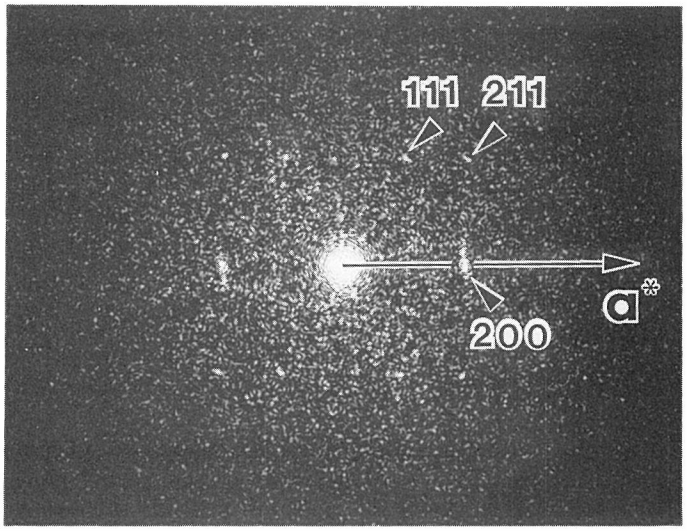

Fig. 9. Optical diffractogram of the high resolution micrograph of a PPS solution-grown crystal tilted around the **a**-axis.

photograph was obtained from a small area of the negative which was reduced to a portion of 50 nm in diameter on the real specimen, there seems to be only one fibrillar crystal in the area. From the obtained reflections, it is considered that the incident direction of electrons is parallel to the $\langle 0\bar{1}1 \rangle$ direction of the crystal. This means that the lattice image is taken from the crystal tilted at an angle of 28.7° around the **a**-axis.

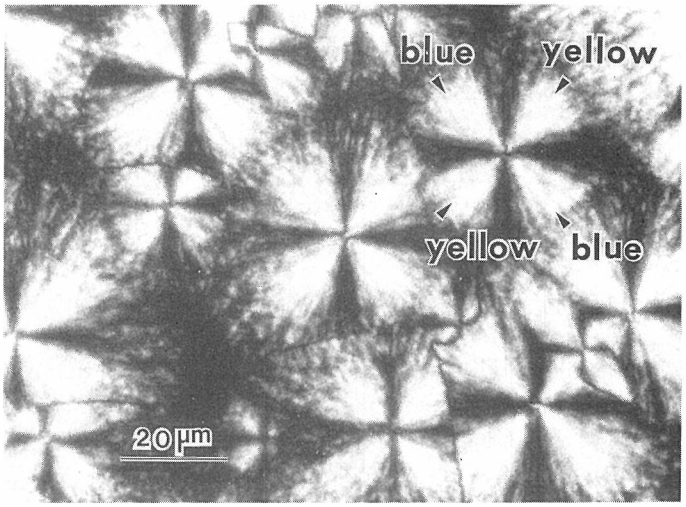

Fig. 10. Polarizing microscopic image of the crystalline thin film with the spherulitic structure which was observed between crossed polars. When a sensitive colour plate is inserted from the lower right-hand to the upper left-hand, the upper right-hand and the lower left-hand sections of the four sections which were divided by the Maltese cross are yellow, and the upper left-hand and the lower right-hand sections are blue, as shown in the figure.

2) *Crystalline thin films with spherulitic structure*

Figure 10 shows the polarizing microscopic image of the crystalline thin film with the spherulitic structure which was observed between crossed polars. When a sensitive colour plate was inserted from the lower right-hand to the upper left-hand on Fig. 10, the upper right-hand and the lower left-hand sections of the four sections which were divided by the Maltese cross were yellow, the upper left-hand and the lower right-hand sections were blue, and the Maltese cross was coloured in red. This result means that this spherulite is optically negative as a polyethylene spherulite[12]. Here the word of 'negative' implies that the crystal axis with a larger refractive index is oriented in the

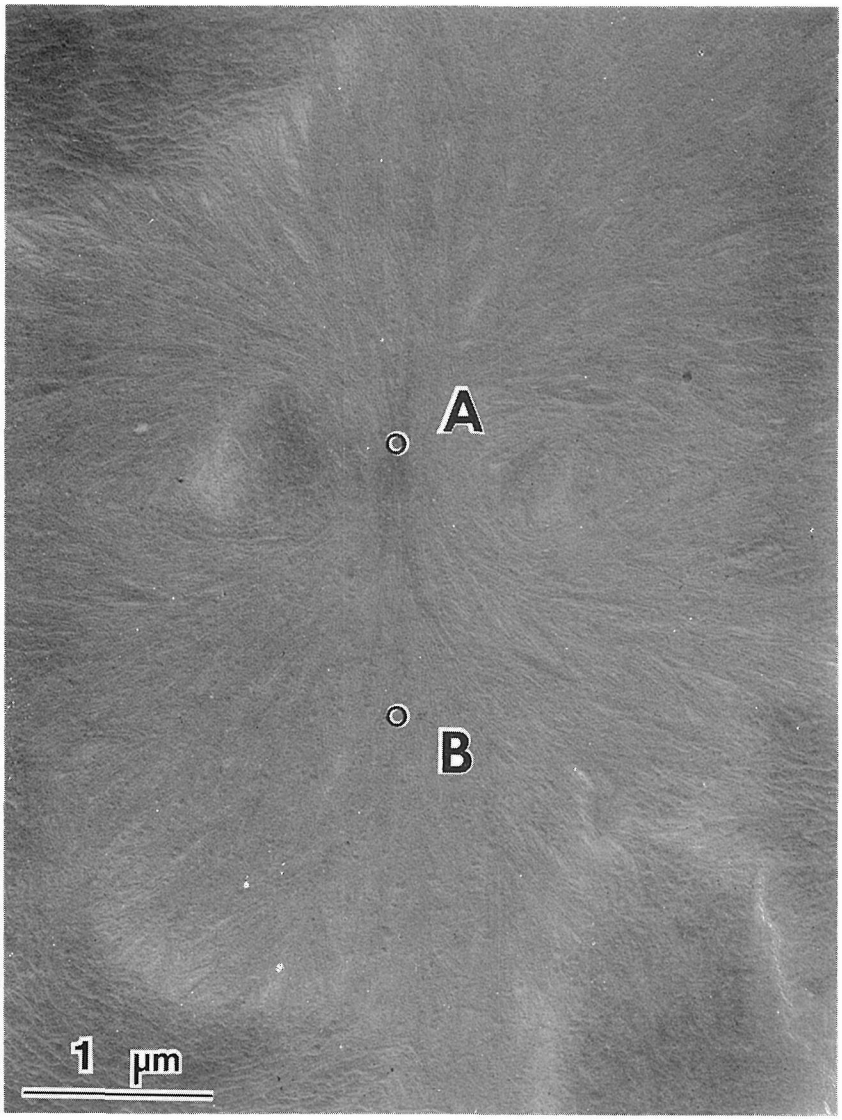

Fig. 11. PPS thin film with spherulitic structure, shadowed with Pt-Pd. A shows the area including the center of the spherulite and B shows the other place than it.

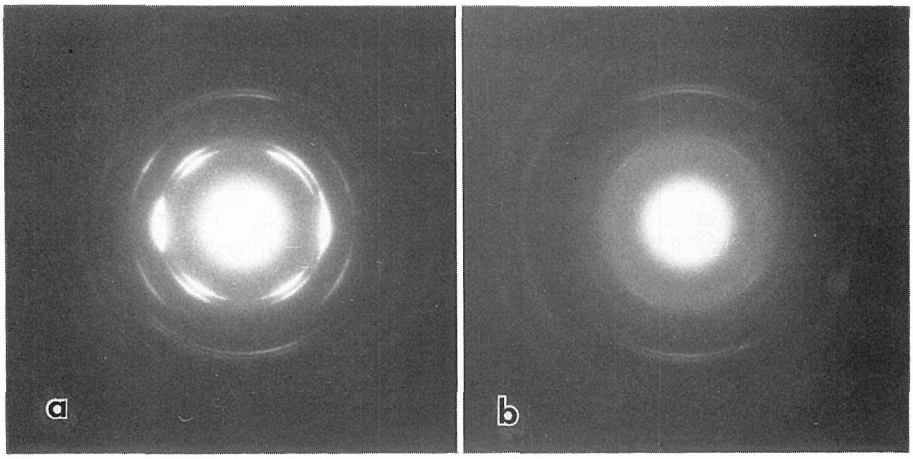

Fig. 12. (a) is the electron diffraction pattern of Fig. 11A, and (b) is that of Fig. 11B. The direction of these figures is the same as that of Fig. 11.

tangential direction of the spherulite, namely, the molecular axis is perpendicularly aligned to the radial direction.

Figure 11 shows the electron microscopic image of PPS thin film. Figure 12(a) is the electron diffraction pattern obtained from the area including the center of a spherulite, and Fig. 12(b) is that obtained from the other place than it. These patterns are different from one another. The pattern (a) is almost the same as the pattern of solution-grown crystals (see Fig. 2), and so within the area around the center of the spherulite, the molecular chains may be normal to the surface of PPS film. From the analysis of the pattern of Fig. 12(b), the **c**-axis is found to be parallel to the tangential direction of spherulite. This is coincident with the fact that this spherulite is negative one. Furthermore, from the fact that the **b**-axis is parallel to the radial direction, it is found that the growing direction of the crystal is in the **b**-axis, as is the case of solution-grown crystal.

CONCLUDING REMARKS

We have obtained solution-grown crystals of PPS. The growing direction of the crystal corresponds to the **b**-axis, and the molecular axis (**c**-axis) is fundamentally vertical to the basal plane of the crystal. We have obtained the high resolution electron microscopic images of the crystal, which resolve some lattice fringes. From the success in taking lattice images of PPS crystals, it is expected to observe directly the lattice defects in PPS crystals. In the case of the doped PPS, it is expected that its structure could be revealed through the direct observation of dopant atoms together with PPS crystal-lattice fringes. The investigation is in progress to elucidate the irregular structure of PPS as such.

Crystalline thin films of PPS were also obtained. They have the spherulitic structure and the spherulite is found to be optically negative through polarizing microscopic observation. The structure of the doped thin PPS-film will be given elsewhere.

ACKNOWLEDGEMENT

We are grateful to Dr. K. Ishizuka of Institute for Chemical Research, Kyoto University for permission to use the program for the computer simulation of electron microscopic image.

REFERENCES

(1) Y. Watanabe, *Kobunshi* (*High polymer*), **33**, 765 (1984).
(2) B. J. Tabor, E. P. Magré and J. Boon, *Eur. Polym. J.*, **7**, 1127 (1971).
(3) K. Katayama, S. Isoda, M. Tsuji, M. Ohara and A. Kawaguchi, *Bull. Inst. Chem. Res., Kyoto Univ.*, **62**, 198 (1984).
(4) M. Tsuji, A. Uemura, M. Ohara, A. Kawaguchi, K. Katayama and J. Petermann, Submitted for publication in *Sen-i Gakkaishi*.
(5) M. Tsuji, S. Isoda, M. Ohara, A. Kawaguchi and K. Katayama, *Polymer*, **23**, 1568 (1982).
(6) A. Kawaguchi, M. Tsuji, S. Moriguchi, A. Uemura, S. Isoda, M. Ohara, J. Petermann and K. Katayama, *Bull. Inst. Chem. Res., Kyoto Univ.*, **64**, 54 (1986).
(7) A. Kawaguchi, S. Isoda, J. Petermann and K. Katayama, *Colloid & Polym., Sci.*, **262**, 429 (1984).
(8) S. Isoda, A. Kawaguchi, A. Uemura and K. Katayama, *Japanese J. Appl. Phys.*, **24**, 341 (1985).
(9) Y. Fujiyoshi, T. Kobayashi, K. Ishizuka, N. Uyeda, Y. Ishida and Y. Harada, *Ultramicroscopy*, **5**, 459 (1980).
(10) M. Tsuji, S. Isoda, M. Ohara, K. Katayama and K. Kobayashi, *Bull. Inst. Chem. Res., Kyoto Univ.*, **55**, 237 (1977).
(11) K. Ishizuka and N. Uyeda, *Acta Cryst.*, **A33**, 740 (1977).
(12) B. Wunderlich, "*Macromolecular Physics*", **Vol. 1**, Academic Press, London, 334 (1973).